Molecular-state study of He^{2+}-H(1s) and H^+-He^+(1s) collisions

M. Kimura*† and W. R. Thorson
Department of Chemistry, University of Alberta, Edmonton, Alberta, Canada T6G 2G2
(Received 30 March 1981)

We have computed direct and charge-exchange excitation cross sections for (a) He^{2+}-H(1s) collisions at projectile energies 1—20 keV, and for (b) H^+-He^+(1s) collisions at c.m. energies 1.6 to 8 keV, using the close-coupling method with HeH^{2+} molecular states as basis and electron translation-factor corrections based on molecular-state switching functions. Basis sets with up to 10 and 12 molecular states have been used, and good convergence of results as a function of basis size is found. The results are compared with recent theoretical calculations of Winter, Lane, and Hatton and with experimental values. For process (a) total charge-transfer cross sections are in generally good agreement with those found by Winter *et al.* using Bates-McCarroll translation factors and, less quantitatively, so are individual state cross sections for $He^+(2s,2p_0,2p_{\pm1})$. For process (b) significant differences with the results of Winter *et al.* are found; these appear to be traceable to the different treatments of the electron translational factors used. Charge-transfer cross sections of Winter, Hatton, and Lane [Phys. Rev. A 22, 930 (1980)] are 14—32 % higher than those found here using comparable basis sets, and individual state cross sections for direct excitation to $He^+(2s,2p_0,2p_{\pm1})$ are also systematically larger than ours (by as much as a factor of 2 in some cases), although values for individual states are only poorly converged in both calculations. Very good agreement is found in all cases with recent experimental measurements.

I. INTRODUCTION

It is now widely recognized that calculations employing molecular-state basis functions are the most appropriate theoretical approach to ion-atom collisions at low to intermediate energies. However, applications have been complicated by difficulties and ambiguities, mostly associated with the effects of electron translation factors (ETF's), which are overlooked by the usual perturbed-stationary-states method; the true validity of the molecular-state approach has been partly obscured by unphysical predictions arising from this defect of perturbed-stationary-state (PSS) theory. Careful studies on prototype systems are therefore still useful to establish the domain of validity.

The one-electron HeH^{2+} collision system is one such prototype, for which a number of theoretical,[1—7] as well as experimental,[7—14] studies have been made. Pioneering work by Piacentini and Salin[1,2] on charge transfer in He^{2+}-*H*(1s) collisions was followed by an extensive benchmark study of Winter and Lane,[3] who included up to 20 molecular states and examined convergence of the results as function of basis size. In both these calculations the proton was taken as reference origin for the electron, and, as in PSS theory, translation factor effects were entirely neglected. Winter and Hatton[4(a),4(b)] have studied the same problem, but including a description of ETF effects; they used "plane-wave" translation factors as defined by Bates and McCarroll.[15] Their results show that translation factor effects are important: Total charge-transfer cross sections show much more rapid convergence with increasing basis size, and the "converged" results are 7—30 % larger than those of Winter and Lane. Finally, Winter, Hatton, and Lane[5] have carried out a study of charge transfer and direct excitation in H^+-He^+(1s) collisions, again using Bates-McCarroll ETF's.

Bates-McCarroll ETF's are appropriate for one-center (atomic) functions. In an asymmetric system like HeH^{2+}, each molecular state is correlated asymptotically ($R\to\infty$) to a single atomic state; hence associating the corresponding Bates-McCarroll ETF for that center with the molecular state (as was done in Refs. 4 and 5) will ensure translational invariance of the results and remove all *asymptotic* defects of the PSS method. However, in a *molecular* state which may have *two-center*

character, a single-center ETF is inappropriate, and its use may lead to incorrect couplings and cross sections. In HeH^{2+}, some of the states (e.g., $1s\sigma$, $2p\pi$) are "He^+-like" at essentially all internuclear separations, but others—primarily those asymptotically correlating to H(nl) (e.g., $2p\sigma$)—have substantial two-center character at smaller R values where coupling occurs.

Thorson and Delos[16] have shown that a rigorous description of ETF effects appropriate to molecular states can be formulated using switching functions;[17,18] in effect, a switching function describes electron translation as a local function of electron position with the molecule. That such detailed descriptions of ETF effects are sometimes necessary has been illustrated clearly in studies of couplings to continuum states.[18–20]

Vaaben and Taulbjerg[6] have reported a study of charge exchange in He^{2+}-H($1s$) collisions using ETF's based on a switching function; their switching function is the *same for all the molecular states* and is derived from arguments based on the molecular Hamiltonian.[21] Their reported values for total charge-exchange cross sections are 50% smaller than those reported by Winter and Hatton[4a,b] at lower energies, and they also report a more rapid convergence. However, (a) we have performed a three-state calculation using their switching function at 1 keV, and obtain a result in good agreement with those reported in Refs. 3 and 4 and with those we have found here (see Sec. III), (b) there is a great deal of evidence[18–20,22,23] suggesting that *different* switching functions should be used for different molecular states. Delos and Thorson[22] have extended their formulation to allow for this possibility (within a classical trajectory treatment of collisions; a fully quantum mechanical formulation has recently been given by Delos[24]).

Recently, Thorson *et al.*[23] have shown that analytical switching functions can be derived from a two-center decomposition of the exact molecular states of H_2^+, and that these switching functions are in *quantitative* agreement with those found earlier by Rankin and Thorson[20] using a heuristic "optimization" of continuum couplings. [We have used these switching functions to perform cross-section calculations for H^+-H($1s$) collisions (1–7 keV),[25] and our results show improved agreement with available recent experiments (relative to previous calculations).] The same ideas may be extended to an asymmetric system such as the HeH^{2+} system[23]. For states with recognizable two-center character (e.g., $2p\sigma$,$3d\sigma$,$3d\pi$, etc.) the analytically derived switching functions are in reasonable (though less quantitative) agreement with those found by optimization studies of both continuum and discrete couplings[26]; the coupling matrix elements obtained by the two methods are in quantitative agreement ($<2\%$ discrepancies at peak maxima). The switching functions used have the form

$$f_n = \tanh[\beta_n R(\eta - \eta_n^0)], \tag{1}$$

where $\eta = (r_A - r_B)/R$ is the "angle" variable of prolate spheroidal coordinates and $\beta_n(R)$, $\eta_n^0(R)$ are R-dependent parameters characteristic of the molecular state n. In the studies reported here we have used parameters found by the optimization scheme (see Table I; cf. also Ref. 26).

Using these switching functions we have performed coupled molecular-state calculations of direct and charge-exchange cross sections for the following collision processes in the HeH^{2+} system:

(a) He^{2+}-H($1s$) collisions for projectile energies 1–20 keV, using up to 12 molecular states;

(b) H^+-He^+($1s$) collisions for relative (c.m.) energies 1–8 keV, using up to 10 molecular states;

Our results may be compared with those of Winter and Hatton[4(a),4(b)] [process (a)] and Winter, Hatton, and Lane[5] [process (b)], and with recent experimental values.[8–12] A brief summary of the main points is as follows.

(1) For process (a), total charge-transfer cross sections (Table III) and less quantitatively, individual state cross sections, are in generally good agreement with those of Winter and Hatton, and converge somewhat more rapidly as a function of basis size, especially at low energies.

(2) For process (b), total charge-transfer cross sections are only in fair agreement with those of Winter *et al.*; the latter are 14–32% larger than our values for comparable basis sets (five-state and ten-state bases). The values reported by Winter *et al.* for individual state cross sections for direct excitation to $He^+(2s, 2p_0, 2p_{\pm 1})$ are also systematically larger than ours (as much as a factor of 2 in some cases). The differences are traceable to diferrences in the treatment of ETF effects and the resulting coupling matrix elements.

(3) Good agreement is found with available experimental values in all cases.

Section II gives a brief account of the method used. Results for He^{2+}-H($1s$) collisions are discussed in Sec. III and those for H^+-He^+($1s$) collisions in Sec. IV.

TABLE I. HeH^{2+} switching function parameters β_n, η_n^0, $f_n(\vec{r},R)=\tanh[\beta_n R(\eta-\eta_n^0)]$.

State	Parameter	R (a.u.) 2.0	4.0	6.0	8.0	10.0	12.0
$1s\sigma$	β	0.844	0.918	0.948	0.964	0.973	0.975
	η^0	0.952	0.885	0.894	0.896	0.906	1.02
$2s\sigma$	β	0.554	0.548	0.541	0.539	0.537	0.533
	η^0	1.84	1.46	1.33	1.25	1.19	1.17
$2p\sigma$	β	0.411	0.361	0.341	0.328	0.322	0.325
	η^0	0.732	0.278	0.076	−0.145	−0.226	−0.332
$2p\pi$	β	0.364	0.371	0.392	0.423	0.437	0.448
	η^0	1.37	0.970	0.878	0.798	0.828	0.837
$3d\sigma$	β	0.232	0.257	0.266	0.274	0.282	0.286
	η^0	1.83	0.724	0.513	0.484	0.485	0.506

II. DETAILS OF METHOD

Assuming nuclear motion is described classically by $\vec{R}(t)$, we solve the resulting time-dependent Schrödinger equation for the electron; the state vector is expanded in an ETF-modified molecular-state basis,

$$\Psi(\vec{r};t)=\sum_n a_n(t)\phi_n(\vec{r};\vec{R}(t))\exp\left[\frac{im}{2\hbar}\vec{v}\cdot\vec{r}f_n(\vec{r};\vec{R})\right]\exp\left[-\frac{i}{\hbar}\int^t\left[\epsilon_n(t')+\frac{mv^2}{8}\right]dt'\right]. \tag{2}$$

Here $\vec{v}=d\vec{R}/dt$ is the relative nuclear velocity, and $\phi_n(\vec{r};\vec{R})$ are the molecular eigenstates of the electronic Hamiltonian $H_{el}(\vec{r};\vec{R})$,

$$H_{el}(\vec{r};\vec{R})\phi_n(\vec{r};\vec{R})=\epsilon_n(r)\phi_n(\vec{r};\vec{R}), \tag{3}$$

which depend parametrically on $\vec{R}$. [In Eq. (2), the reference origin for electron coordinates $\vec{r}$ is the *geometric* center, not the center of mass of the nuclei[22]; with respect to this point the nuclei have velocities $\pm\frac{1}{2}\vec{v}$, respectively.] Substituting Eq. (2) in the Schrödinger equation, multiplying by

$$\phi_k^*\exp[-(im/2\hbar)\vec{v}\cdot\vec{r}f_k],$$

and integrating over electron coordinates yields coupled equations for the coefficients $a_n(t)$; after expanding in powers of velocity $\vec{v}$, one obtains[22]

$$i\hbar\dot{a}_k(t)=\sum_{n\neq k}\vec{v}\cdot(\vec{P}+\vec{A})_{kn}a_n(t)\exp\left[-\frac{i}{\hbar}\int^t(\epsilon_n-\epsilon_k)dt'\right] \tag{4}$$

to first order in $\vec{v}$, where

$$\vec{P}_{kn}=\langle\phi_k\,|\,-i\hbar\vec{\nabla}_R\,|\,\phi_n\rangle \tag{5}$$

and

$$\vec{A}_{kn}=(im/\hbar)\langle\phi_k\,|\,[H_{el},\vec{s}_n]\,|\,\phi_n\rangle \tag{5b}$$

$$=(im/\hbar)(\epsilon_k-\epsilon_n)\langle\phi_k\,|\,\vec{s}_n\,|\,\phi_n\rangle \tag{5c}$$

with

$$\vec{s}_n=\tfrac{1}{2}f_n(\vec{r};\vec{R})\vec{r}. \tag{5d}$$

We have tested the accuracy of the first-order equations for this problem by computing individual state probabilities for process (a) at 20 keV (4 keV in c.m. frame) and a number of impact parameters, with the four-state basis ($2p\sigma$, $2p\pi$, $3d\sigma$, $2s\sigma$), using coupled equations accurate to second order in velocity [these equations are given in Eq. (4) of Ref. 25]. The results change by at most 1% in all cases. [We have not made tests for process (b) at the higher energy of 8 keV (c.m. system); however, we have found from extensive second-order calculations in the H^+-H(1s) collision system, where the second-order effects *are* significant,[25] that the

second-order effects increase in roughly linear fashion with increasing energy. This suggests that errors of about 2% in individual state probabilities may be expected due to neglect of second-order terms in process (b) at 8 keV.]

We used straight-line trajectories $\vec{R}(t)$, since it was found in Refs. 3–5 that this is a reasonable approximation, with at most 8% error at 1 keV.

The couplings may be divided into radial and angular parts,

$$\vec{v}\cdot(\vec{P}+\vec{A})_{kn}=\dot{R}(P^R+A^R)_{kn}+R\dot{\theta}(P^\theta+A^\theta)_{kn}\,, \tag{6}$$

where

$$P^R_{kn}=-i\hbar\left\langle k\left|\left[\frac{\partial}{\partial R}\right]_{\vec{r}}\right|n\right\rangle \tag{7a}$$

$$=-i\hbar(\epsilon_n-\epsilon_k)^{-1}\left\langle k\left|\left[\frac{\partial H_{\rm el}}{\partial R}\right]_{\vec{r}}\right|n\right\rangle$$

and

$$P^\theta_{kn}=-R^{-1}\langle k\,|\,\hat{L}_y\,|\,n\rangle \tag{7b}$$

are the usual (uncorrected) radial- and angular-coupling matrix elements in PSS theory ($\hat{L}_y$ is the electronic angular-momentum component perpendicular to the collision plane, relative to the geometric center). The ETF corrections A^R,A^θ are given, respectively, by the components of (5c) parallel and perpendicular to $\vec{R}$. We employed switching functions of the form of Eq. (1); the parameters β_n,η_n^0 were determined by the optimization studies described earlier[20,26,23]; their values for $1s\sigma$, $2s\sigma$, $2p\sigma$, $3d\sigma$, and $2p\pi$ states are given in Table I.

Exact molecular eigenstates ϕ_n and eigenvalues $\epsilon_n(R)$ were generated by the method of Bates and Carson.[27] Coupling matrix elements were evaluated using Gauss-Legendre and Gauss-Laguerre quadratures with relative errors $<1\times10^{-6}$.

Figure 1 shows $\epsilon_n(R)$ versus R for 22 molecular states of HeH^{2+}. In Table II are listed basis sets used. For process (a), most calculations were done using the four- and ten-state bases; for process (b), the five- and ten-state bases were used. The 12-state set was used to make some checks on convergence of the total charge-transfer cross sections and for some studies of excitation probabilities [especially H($n=2$) levels] at selected energies and impact parameters.

Our ten-state basis differs from that employed in Refs. 4 and 5; we have deleted the states $3s\sigma$, $3d\delta$

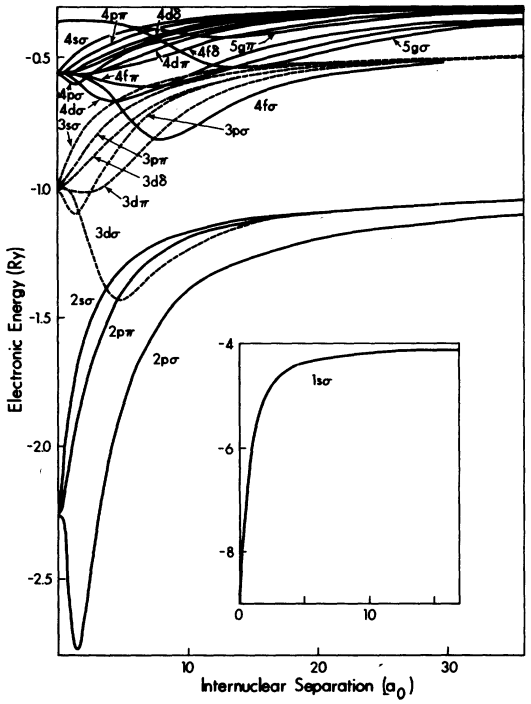

FIG. 1. Electronic energy $\epsilon_n(R)$ (in Ry) versus R, for 22 molecular states of HeH^{2+}.

and added the states $4d\sigma$, $4f\pi$, which correspond asymptotically to H($n=2$) + He^{2+}. Reasons for this choice were that (a) it appears from Ref. 4, and also from our own preliminary studies, that the states $3s\sigma$ and $3d\delta$ play a relatively insignificant part in the processes studied, and (b) inclusion of $4d\sigma$ and $4f\pi$ allows us to make some estimate of charge transfer to H($n=2$) levels in process (b).

Taking $a_k(-\infty)=\delta_{k1}$, where "1" designates the initial state, final amplitudes $a_k(+\infty;\rho)$ were computed by numerical integration of Eq. (4) for a suitable range of impact parameters; we used the method of Bulirsch and Stoer,[28] with a relative truncation error automatically maintained between 1×10^{-4} and 1×10^{-6}. Conservation of probability was maintained to within $1\times10^{-4}-1\times10^{-5}$. The probability of excitation to the molecular state k is

$$P_k(E,\rho)=|\,a_k(+\infty;\rho)\,|^2 \tag{8}$$

and the corresponding integrated cross section is

$$Q_k(E)=2\pi\int_0^\infty \rho\,d\rho\,P_k(E,\rho)\,. \tag{9}$$

Asymptotic couplings. Within an asymptotically degenerate atomic manifold—such as the He^+ ($n=2$) manifold of $2s\sigma$, $3d\sigma$, and $2p\pi$ states—a long-range-coupling problem arises which we found

TABLE II. HeH^{2+} molecular-state basis sets for He^{2+}-H(1s) and H^+-He^+(1s) collisions.

Numbers of states in basis	Basis states	Limiting atomic levels
3	$2p\sigma$	$H(1s) + He^{2+}$
	$2p\pi, 3d\sigma$	$H^+ + He^+(n=2)$
4	as above, plus	
	$2s\sigma$	$H^+ + He^+(n=2)$
5	as above, plus	
	$1s\sigma$	$H^+ + He^+(1s)$
10	as above, plus	
	$3p\sigma, 3p\pi, 3d\pi$	$H^+ + He^+(n=3)$
	$4d\sigma, 4f\pi$	$H(n=2) + He^{2+}$
12	as above, plus	
	$4f\sigma$	$H^+ + He^+(n=3)$
	$5g\sigma$	$H(n=2) + He^{2+}$

convenient to treat separately. The two hybrid (sp) σ states are linked to $2p\pi$ by Coriolis coupling and to each other by radial coupling. Neither R or t is a suitable progress variable, since both couplings and splittings decrease only as R^{-2}. For $R \geq 16$ a.u. both couplings and splittings can be accurately modeled by analytical perturbation expressions, and using the action variable

$$\zeta = \int_{\infty}^{t} \frac{\rho v_0 dt'}{R^2}$$

as progress variable the problem may be solved very efficiently. Its solution generates a three-state propagator $U(\infty; R_0)$ which converts molecular-state amplitudes at R_0 (boundary of the "real collision" region, $\simeq$16 a.u.) to those at $R \to \infty$. The effects of this coupling are significant; for example, at 8 keV, the cross sections for $He^+(2s)$ excitation as computed by this procedure differ by about 25% from those found by direct numerical integration of Eq. (4) even as far as $R=25$ a.u.

Coherence effects. The molecular states $2s\sigma$ and $3d\sigma$ correspond asymptotically to (sp) hybrid atomic levels of $He^+(n=2)$; to compute probabilities and cross sections for $He^+(2s)$ and $He^+(2p_0)$ *atomic states,* the corresponding amplitudes must be formed by coherent addition of (Schrödinger picture) amplitudes for the $2s\sigma$, $3d\sigma$ molecular states [cf. Eq. (11) and Ref. 25]

He^{2+}-*H*(1*s*) COLLISIONS

Figures 2 and 3 compare our matrix elements for the dominant $2p\sigma \leftrightarrow 2p\pi$ and $2p\sigma \leftrightarrow 3d\sigma$ couplings (solid curves) with those obtained using Bates-McCarroll ETF's, (and also those computed with the universal switching function of Vaaben and Taulbjerg). The differences with the plane-wave ETF couplings are substantial, especially for the $2p\sigma \leftrightarrow 3d\sigma$ radial couplings.

Just as for H^+-H(1s) collisions,[25] the primary excitation path is the strong $2p\sigma$-$2p\pi$ rotational coupling associated with orbital degeneracy in the united atom, but an important secondary mechanism, particularly at larger impact parameters, arises from the radial $2p\sigma \to 3d\sigma$ coupling. $3d\sigma$-$2p\pi$ Coriolis coupling (not shown) is one of the asymptotic couplings within the $He^+(n=2)$ manifold ($2s\sigma$, $2p\pi$, $3d\sigma$), which we treat specially beyond

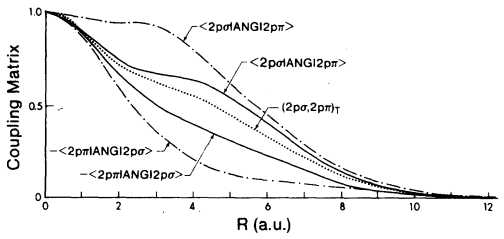

FIG. 2. ETF-corrected $2p\sigma \leftrightarrow 2p\pi$ angular-coupling matrix elements computed using different ETF descriptions. The angular-coupling operator (denoted "ANG") is the sum of the PSS coupling, Eq. (7b), and the ETF correction whose matrix elements are A^{θ} [see Eq. (5c)]. Solid curves, present work; —·—·—·, based on Bates-McCarroll ETF's (Ref. 4); · · · , based on switching function of Vaaben and Taulbjerg (Ref. 6).

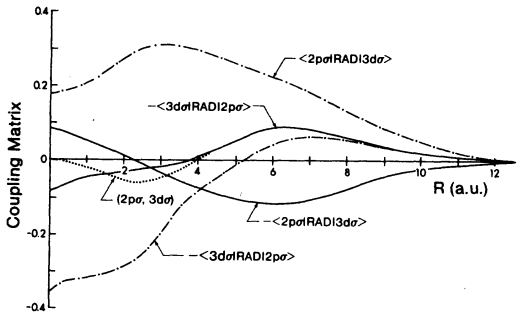

FIG. 3. ETF-corrected $2p\sigma \leftrightarrow 3d\sigma$ radial-coupling matrix elements computed using different ETF descriptions. The radial-coupling operator (denoted "RAD") is the sum of the PSS coupling, Eq. (7a), and the ETF correction whose matrix elements are A^R [see Eq. (5c)]. Solid curves, present work; —·—·—·, based on Bates-McCarroll ETF's (Ref. 4); · · ·, based on switching function of Vaaben and Taulbjerg (Ref. 6).

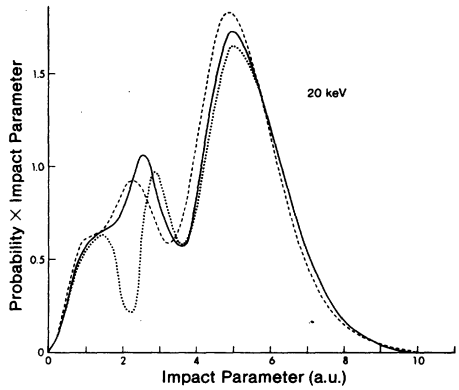

FIG. 5. Probability of charge transfer times impact parameter $[\rho P_{ex}(\rho)]$ versus impact parameter for He^{2+}-H(1s) collisions at 20 keV. ——, present ten-state results; -----, ten-state results of Winter and Hatton [Ref. 4(a)]; · · · ·, present five-state results.

$R = 16.0$ a.u., but it also has significant effects at shorter distances. A "collision history" plot (not shown) similar to those given by Piacentini and Salin[2] would illustrate all these effects in sequence. Figure 4 shows probabilities for $2p\pi$, $3d\sigma$, and $2s\sigma$ molecular states versus impact parameter at 8 keV. The united-atom $2p\sigma$-$2p\pi$ coupling produces the $2p\pi$ peak at small impact parameters. The Rosen-Zener-Demkov oscillatory peak structure for $3d\sigma$ is produced by $2p\sigma$-$3d\sigma$ radial coupling, and the relatively small $2p\pi$ peaks at larger impact parameters, which are in phase with those for $3d\sigma$, are produced indirectly, via $3d\sigma$, by the $3d\sigma$-$2p\pi$ angular coupling. The small $2s\sigma$ peak for $\rho < 1$ is produced by $2p\sigma$-$2s\sigma$ radial coupling which has a maximum at small R and falls off sharply for $R > 2$ a.u.

Figure 5 shows total charge-transfer probability times impact parameter versus impact parameter, at 20 keV, for our four- and ten-state basis calculations, and, for comparison, the ten-state results of Winter and Hatton[4(a)] (data kindly supplied to us by Dr. T. G. Winter). It is interesting that in spite

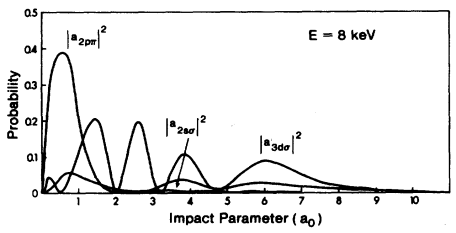

FIG. 4. Molecular-state excitation probabilities versus impact parameter for He^{2+}-H(1s) collisions at 8 keV.

of the rather different coupling matrix elements shown in Figs. 2 and 3, the agreement between the two sets of ten-state results is generally good. Even better agreement (as to phases and amplitudes of observed peaks) is found with Ref. 4(a) at lower collision energies.

As noted in Refs. 3 and 4, the four states $2p\sigma$, $2p\pi$, $3d\sigma$, $2s\sigma$ are almost adequate to study charge transfer in process (a) at these energies, since $He^{2+} + H(1s)$ and $He^+(n=2) + H^+$ are near-resonant levels. It is more difficult to decide in advance which of the more highly excited states will contribute appreciably to secondary effects. In making choices we used information from the earlier studies[3-5] as well as preliminary studies of couplings using switching function ETF's. Inclusion of the states $3p\sigma$, $3p\pi$, $3d\pi$ is important because these states are significantly coupled to $3d\sigma$. As noted above, we chose to omit $3s\sigma$ and $3d\delta$ since these seem to be only weakly coupled to the lower levels. We included instead the $4d\sigma$ (coupled to $3p\pi$, $3d\pi$) and $4f\pi$ states, which are correlated to $H(n=2) + He^{2+}$. For a further study of convergence as function of basis size, we did calculations at 8 and 20 keV, for eight to ten values of impact parameter, using the 12-state set formed by adding $4f\sigma$ and $5g\sigma$ to the ten-state set.

Total charge-transfer cross section. Table III shows our results for three-, four-, and ten-state bases, together with results of previous calculations.[1-4,6] There is generally good agreement at all energies between our results and those of Hatton, Lane, and Winter[4(b)] [cf. also Ref. 4(a)] who used Bates-McCarroll ETF's; like them we find

TABLE III. Total charge-transfer cross sections: $He^{2+} + H(1s) \rightarrow He^{+} + H^{+}$ (units 10^{-16} cm^2).

Calculation	Basis size	He^{2+} Energy (keV) 1	3	8	20
Piacentini and Salin (Ref. 2) (1977)	3	0.238	0.985	3.27	5.36
Winter and Lane (Ref. 3) (1978)	3	0.238	0.994	3.27	5.34
	10	0.247	1.03	3.80	7.20
	20		1.22	4.66	9.37
Vaaben and Taulbjerg (Ref. 6) (1979)	3	0.134	1.25	5.40	10.36
	10	0.135	1.26	5.19	9.63
Hatton, Lane, and Winter (Ref. 4) (1980)	3	0.247	1.45	5.93	10.1
	4	0.264	1.49	6.07	10.8
	10	0.265	1.49	6.30	12.2
Kimura and Thorson (1981)	3	0.258	1.40	5.90	9.85
	4	0.260	1.43	6.01	10.40
	10	0.260	1.43	6.15	11.23

that convergence of the results as function of basis size is much improved (relative to the PSS results of Winter and Lane[3]), when ETF effects are included. Setting aside for the moment the results reported by Vaaben and Taulbjerg,[6] it also appears that the convergence *limits* of the ETF-corrected calculations are significantly different from those of the uncorrected calculations, at least at the higher energies.

The results reported by Vaaben and Taulbjerg,[6] using a common switching function for all molecular states, are in marked disagreement with our values and those of Hatton, Lane, and Winter,[4(b)] especially at the lowest energies, where the effects of ETF corrections appear to be least significant for this system and where all other calculations reported in Table III agree most closely. These results were sufficiently disturbing that we performed a calculation at 1 keV using their switching function. For the three-state basis at 1 keV we find the value 0.247×10^{-16} cm^2, in general agreement with other values in Table III.[29]

At 8 and 20 keV the convergence of our total cross sections is somewhat faster than that of Ref. 4 (changes from four-state to ten-state basis cross sections are 64% of those of Ref. 4, in both cases); however, the comparison is not clear cut, since the ten-state bases differ slightly. Additional information about convergence is provided by results of calculations using 12 basis states at 8—10 values of impact parameter (1—10 a.u.), for both energies: in every case the total charge-transfer probability changed by less than 1% relative to the ten-state basis result. At 20 keV, it also appears that the convergence *limit* resulting from the two ETF treatments might be slightly different as well, though calculations using still larger basis sets would be needed to settle that question.

Figure 6 compares ten-state results of ourselves

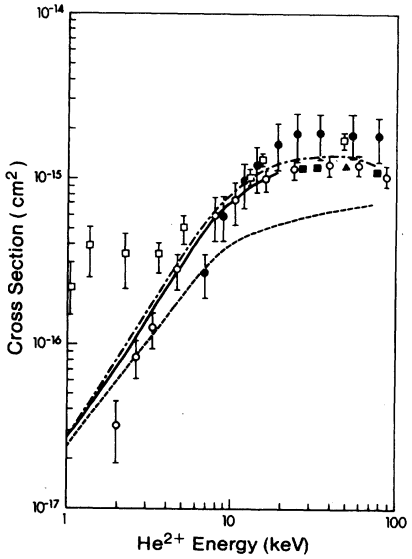

FIG. 6. Total charge-transfer cross section for $He^{2+} + H(1s)$ collisions, versus projectile energy E. Theoretical results: ——, present work; — — —, Hatton, Lane, and Winter (Ref. 4); --------, Piacentini and Salin (Ref. 2). Experimental values: □, Fite *et al.* (Ref. 8); ●, Bayfield and Khayrallah (Ref. 11); ○, Gilbody *et al.* (Refs. 9 and 10); □, Olson *et al.* (Ref. 7).

and of Hatton, Lane, and Winter[4(b)] with experimental values,[7-11] showing that there is excellent agreement between them.

Detailed level cross sections. Cross sections for electron transfer to individual levels $He^+(n)$, $n=1$, 2, 3, and for direct excitation to $H(n=2)$ are shown for the ten-state basis in Table IV. By far the largest contribution to charge transfer comes from the $He^+(n=2)$ manifold due to the near resonance with[30] $H(1s)$—99.2, 95.6, and 93.3 % at 1, 8, and 20 keV, respectively. Capture to the $He^+(1s)$ ground state is unimportant at these energies (0.2 − 1.3 %). A secondary contribution is made to $He^+(n=3)$ (0.6, 2.9, 4.8 %, respectively), and direct excitation of $H(n=2)$ is about 1.5% of the total charge-transfer cross section at 8 and at 20 keV. However, these higher level cross sections may be expected to change significantly if a larger basis set is used. We find, for example, using the 12-state basis set at 8 keV, that population of $H(n=2)$ is increased by ~40%, mainly because the inclusion of $4f\sigma$ greatly increases the $4f\pi$ population via the rotational coupling between them; a secondary effect is introduced by *inclusion* of $5g\sigma$, even though the final $5g\sigma$ population is itself negligible. [Similar effects are mentioned in Ref. 4(b).] Expansion of the basis to include such states as $4d\sigma$, $3d\delta$, $4d\pi$, etc., would be likely to shift upper-level populations back toward $He^+(n=3,4)$ levels again. However, these results do confirm that (when ETF effects are included) the four-state basis is sufficient for a qualitative account of He^{2+}-$H(1s)$ collisions at these energies.

Table V presents an analysis of individual atomic-state cross sections within the $He^+(n=2)$ level. At low energies the principal contribution comes from $2p_{\pm1}$ excitation associated with the $2p\sigma$-$2p\pi$ rotational coupling, but as the energy increases this is overshadowed by the radial $2p\sigma$-$3d\sigma$ coupling, and, to a lesser extent, the $2p\sigma$-$2s\sigma$ coupling which populate the $2s$ and $2p_0$ states. Increase in the basis from four to ten states affects the $2p_{\pm1}$ cross section much less than those for $2s$ and $2p_0$. This happens because a number of higher states (e.g., $3d\pi$) couple strongly with $3d\sigma$ due to its "promotion" in the united atom limit, while the $2s\sigma$ and $2p\pi$ states are relatively isolated from the higher levels (cf. Fig. 1).

Figure 7 shows a comparison of our and other theoretical results for the $He^+(2s)$ cross section with experimental values.[9-11] Our results and those of Winter and Hatton[4] are in good agreement with the experiments, especially those of Gilbody *et al.*[9,10] above 5 keV; as already noted by Winter and Hatton, however, the *energy dependence* at low energies is in better accord with the trend of the measurements of Bayfield and Khayrallah.[11]

IV. H^+-$He^+(1s)$ COLLISIONS

Since $He^+(1s)$ plays a negligible role in He^{2+}-$H(1s)$ collisions, it is not surprising that the total charge-transfer and direct excitation cross sections for H^+-$He^+(1s)$ collisions are very small, as has already been shown by Winter, Hatton, and Lane.[5]

However, in this case we find that the treatment given to ETF corrections has a more significant effect on the values found for these cross sections, using basis sets of comparable size, than is the case for process (a). Our five-state basis and that of Ref. 5 are identical; as noted previously, the two ten-state bases differ slightly, but they do so in respect to states which are relatively weakly and indirectly linked to the more important lower levels.

Figures 8 and 9 compare our coupling matrix elements linking $1s\sigma$ to $2p\sigma$, $2p\pi$, and $2s\sigma$ states with those found by Winter, Hatton, and Lane[5] using Bates-McCarroll ETF's (N.B.: couplings are non-Hermitian only if ETF's for the two states coupled are different. Since $1s\sigma$, $2p\pi$, and $2s\sigma$ all correlate to He^+ states, couplings from Ref. 5 among these are Hermitian). For $1s\sigma \leftrightarrow 2p\sigma$ coupling (Fig. 8), which is of primary importance for

TABLE IV. Atomic level excitation cross sections $He^{2+} + H(1s)$ (units 10^{-16} cm^2) (ten-state basis).

He^{2+} energy (keV)	$He^+(1s)$	$He^+(n=2)$	$He^+(n=3)$	$H(n=2)$
1	4.89×10^{-7}	0.258	1.6×10^{-3}	4.1×10^{-4}
8	2.8×10^{-4}	5.88	0.176	0.094
20	2.5×10^{-3}	10.54	0.535	0.155

TABLE V. $He^{+}(n=2)$ atomic-state cross sections, He^{2+} - H(1s) collisions (units 10^{-16} cm^2).

He^{2+} energy (keV)	Basis size	2s	$2p_0$	$2p_{\pm 1}$
1	4	0.040	0.026	0.194
	10	0.038	0.024	0.195
8	4	1.40	2.66	1.95
	10	1.21	2.65	2.02
20	4	2.65	3.97	3.78
	10	2.18	4.66	3.70

this collision process, our coupling matrix elements are very different from those of Winter *et al.*,[5] especially for $R \lesssim 3$ a.u. where most of the coupling occurs, and it is not surprising that different $2p\sigma$ probabilities result.[31] Some differences among the secondary couplings from $1s\sigma$ (Fig. 9) exist but these are probably less important for cross sections.

Figures 10 and 11 depict collision histories for the five-state basis (cf. Table II) at c.m. energy $E_{\text{c.m.}}=4$ keV and impact parameters 0.5 and 2.p a.u., respectively. The dominant event in both cases is excitation from $1s\sigma$ to $2p\sigma$. At higher energies direct coupling from $1s\sigma$ to $2p\pi$ and (to a smaller extent) from $1s\sigma$ to $2s\sigma$ play some part, but (for example) the peak in $2p\pi$ probability in Fig. 10 results from the two-step process $1s\sigma$-$2p\sigma$-$2p\pi$, rather than direct coupling. Similarly, effects of $2p\sigma$-$3d\sigma$ radial coupling later in the collisions lead to two-step population of $3d\sigma$. A large portion of the flux eventually appearing in $He^{+}(n=2)$ levels thus passes through the "gateway" of the $2p\sigma$ (charge-exchange) state as intermediate. This picture is not significantly altered by going to the ten-state basis, and it would explain why both the charge-transfer cross section and the "direct excitation" cross sections for $He^{+}(n=2)$ should be sensitive to the $1s\sigma$-$2p\sigma$ coupling (this is also the reason why we have presented our results for charge exchange and for direct excitation together, rather than separately).

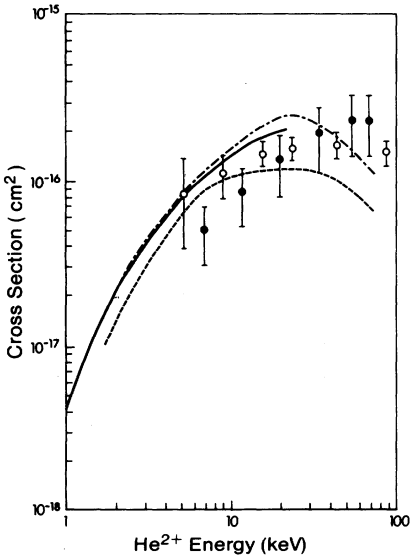

FIG. 7. $He^{+}(2s)$ capture cross section versus E for He^{2+}-H(1s) collisions. Theoretical results: ——, present work; — — —, Winter and Hatton [Ref. 4(a)]; -----, Piacentini and Salin (Ref. 2). Experimental values: ●, Bayfield and Khayrallah (Ref. 11); ○, Gilbody *et al.* (Refs. 9 and 10).

Cross sections. Table VI presents our calculated charge-transfer and direct excitation cross sections for the five-state (KT5) and ten-state (KT10) bases at 1.6, 4, and 8 keV. Also shown for comparison are the values reported by Winter, Hatton, and Lane[5] (WHL5, WHL10); note that for WHL10 no

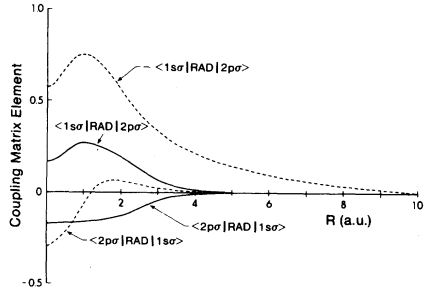

FIG. 8. ETF-corrected $1s\sigma \leftrightarrow 2p\sigma$ radial coupling computed using different ETF descriptions. Radial-coupling operator "RAD" as defined in Fig. 3. Solid curves, present work; dashed curves, couplings based on Bates-McCarroll ETF's (Ref. 5).

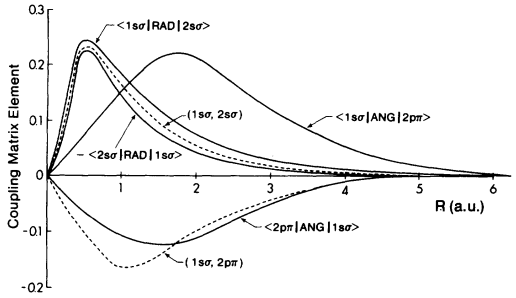

FIG. 9. ETF-corrected radial ($1s\sigma \leftrightarrow 2s\sigma$) and angular ($1s\sigma \leftrightarrow 2p\pi$) coupling using different ETF descriptions. Operators defined "ANG" and "RAD" are defined in Figs. 2 and 3. Solid curves, present work; dashed curves, couplings based on Bates-McCarroll ETF's (Ref. 5).

basis state correlating to H($n=2$) occurs, and that cross sections for $He^+(n=3)$ were not reported in Ref. 5. Our results may be compared with those of Ref. 5 in several ways.

(1) Convergence: For the H(1s) charge-transfer cross sections, the largest change we find in going from the five- to the ten-state basis is -4.3% (8 keV), compared to -7.9% (4 keV) for Ref. 5. For excitation of $He^+(n=2)$ levels, the stability of the individual $2s$, $2p_0$, and $2p_{\pm 1}$ cross sections is much poorer, particularly at 8 keV (changes of $+14$, -26, and -12%, respectively, compared to $+13$, -55, and -19% for Ref. 5). The reason for this instability, of course, is the substantial redistribution of flux into $He^+(n=3)$ and H($n=2$) levels due to coupling from $3d\sigma$ to $3d\pi$, $3p\sigma$, $3p\pi$ (and $4d\sigma$ in our case), when these states are included; that it is $3d\sigma$ which serves as the connection is reflected in the somewhat better stability of $2p\pi$ cross sections. Perhaps a more significant measure of "overall convergence" is given by the changes of

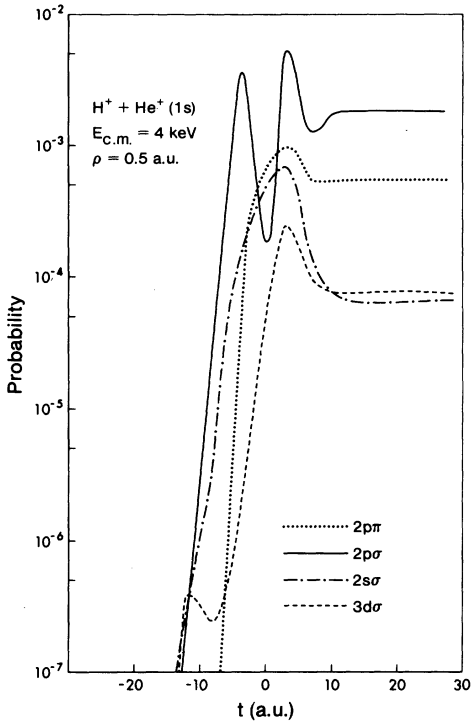

FIG. 10. Collision history (probability versus time) for five-state basis, H^+-$He^+(1s)$ collision at c.m. energy 4 keV, and impact parameter 0.5 a.u.

TABLE VI. Atomic level excitation cross sections for H^+-$He^+(1s)$ collisions (units 10^{-16} cm^2) (Present results: KT5, KT10; results of Ref. 5: WHL5, WHL10).

$E_{c.m.}$ (keV)	Basis and calc.	H(1s)	$He^+(2s)$	$He^+(2p_0)$	$He^+(2p_{\pm 1})$	H($n=2$)	$He^+(n=3)$
1.6	KT5	2.88×10^{-5}	3.68×10^{-6}	3.21×10^{-6}	7.10×10^{-6}		
	KT10	2.82×10^{-5}	3.62×10^{-6}	2.88×10^{-6}	6.92×10^{-6}	2.15×10^{-7}	4.75×10^{-7}
	WHL5	3.41×10^{-5}	6.51×10^{-6}	5.62×10^{-6}	7.95×10^{-6}		
	WHL10	3.23×10^{-5}	6.40×10^{-6}	4.71×10^{-6}	7.40×10^{-6}		
4	KT5	1.98×10^{-3}	2.56×10^{-4}	2.38×10^{-4}	3.56×10^{-4}		
	KT10	1.94×10^{-3}	2.64×10^{-4}	1.87×10^{-4}	3.47×10^{-4}	4.98×10^{-5}	9.72×10^{-5}
	WHL5	2.46×10^{-3}	3.08×10^{-4}	4.06×10^{-4}	4.20×10^{-4}		
	WHL10	2.28×10^{-3}	3.30×10^{-4}	2.66×10^{-4}	4.01×10^{-4}		
8	KT5	9.27×10^{-3}	2.31×10^{-3}	1.37×10^{-3}	2.84×10^{-3}		
	KT10	8.89×10^{-3}	2.67×10^{-3}	1.09×10^{-3}	2.54×10^{-3}	9.62×10^{-4}	1.55×10^{-3}
	WHL5	12.2×10^{-3}	4.70×10^{-3}	2.78×10^{-3}	3.64×10^{-3}		
	WHL10	12.4×10^{-3}	5.39×10^{-3}	1.79×10^{-3}	3.05×10^{-3}		

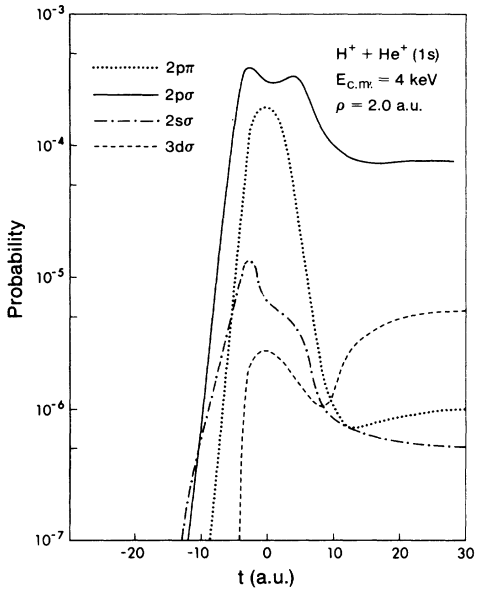

FIG. 11. Collision history for five-state basis, H^+-H(1s) collision at c.m. energy 4 keV, and impact parameter 2.0 a.u.

-1, $+2$, and $+10\%$ (at 1.6, 4, and 8 keV, respectively) in the *total* cross section for both charge transfer *plus* excitations of all kinds: These figures make it clear that augmentation of the basis from five to ten states has *not* caused massive changes in the flux drained from $1s\sigma$. Unfortunately, the corresponding data is not available from Ref. 5.

While it appears that the convergence of our results is slightly faster than that for Ref. 5, a comparison is weakened by the differences in the two ten-state bases. In both cases, further augmentations of the basis may be expected to cause significant changes in the $He^+(n=2)$ individual state cross sections. On the other hand it may be reasonable to expect that the charge transfer to H(1s), and especially the total flux loss from $1s\sigma$, will be much more stable ($\lesssim 10\%$ change at 8 keV?).

(2) Cross-section values. In our opinion, a more significant difference is found in comparisons of the cross-section magnitudes found here with those reported in Ref. 5 (see Table VI), and comparisons of both five-state and ten-state results are relevant for this purpose. In every case, the cross-section values reported by Winter *et al.* are appreciably larger than those we obtain for the comparable basis. For the more stable H(1s) charge-transfer cross section, the cross sections of Ref. 5 are $18-32\%$ larger than ours for the five-state basis, and $14-26\%$ larger than ours for the ten-state basis. These differences are at least twice as large as changes occurring due to basis augmentation in Ref. 5, and at least four times as large as those due to augmentation in our results. While it is conceivable that further, large augmentation of the basis (discrete states only) might lead to reconciliation of these differences, it is our opinion that this will *not* occur. In principle, there is no reason to expect that such convergence on a common value must occur, *unless completeness of the two basis sets is explicitly ensured by inclusion of both continuum and discrete states in each.*

An alternative explanation of these differences, i.e., that they result from effects of higher order terms in the velocity (we retained only first-order terms in our calculation), seems improbable to us because (a) the differences are $18-14\%$ even at 1.6 keV, (b) as stated previously, we studied effects of the second-order terms for process (a) at $E_{c.m.}=4$ keV (20-keV projectile energy) and found them less than 1% for *individual state probabilities,* and (c) the sign of these second-order corrections is always negative—which would increase the observed discrepancies.

Similarly large or even larger discrepancies (as much as a factor of 2 for 2s and $2p_0$, and $17-22\%$ for $2p_{\pm 1}$) occur for the individual direct excitation cross sections. Given the poorer convergence in both sets of calculations for these detailed cross sections, it is not so clear that the values would converge on different limits; however, the consistency of the discrepancies found suggests this as a reasonable possibility.

In summary, the comparisons made above suggest that the different treatments of ETF corrections made by ourselves and by Winter, Hatton, and Lane[5] may lead, for process (b), to significantly *different* cross sections both for charge transfer and for direct excitations, and it is our opinion that this is in fact the case. (It should be possible to test this by calculations using a basis perhaps twice as large as those employed here.)

We do not attribute any particular significance to the specific numbers reported for $H(n=2)$ charge-transfer and $He^+(n=3)$ direct excitation cross sections, as these may be expected to change appreciably when additional states belonging to the same manifold are included in the basis. We do agree with the conclusions of Ref. 5 (based on PSS studies) that the $H(n=2)$ cross section is "small" [$4-10\%$ of $H(n=1)$].

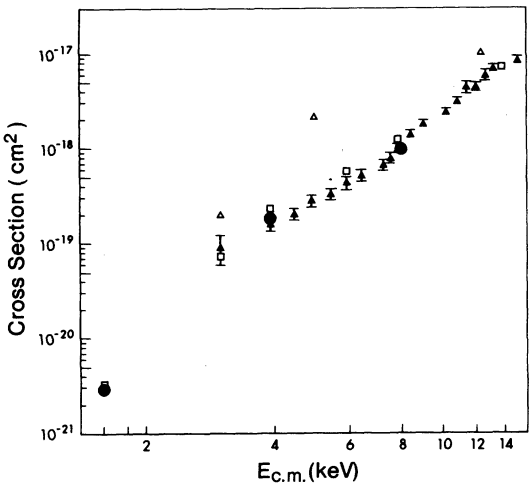

FIG. 12. Total charge-transfer cross section for H^+-$He^+(1s)$ collisions, versus c.m. energy E. Theoretical results: □, Winter, Hatton, and Lane (Ref. 5); △, atomic-state calculations by Rapp (Ref. 32); ●, present work; ▲, experimental values of Peart *et al.* (Ref. 12).

Comparison with experiment. Experimental values for the total charge-transfer cross section, as reported by Peart, Grey, and Dolder,[12] are shown in Fig. 12 together with our ten-state results [including $H(n=2)$], and those of Ref. 5. The experimental values have been determined from the measured He^{2+} formation; hence they include both charge-transfer and ionization events, though it may be reasonable to assume that the contribution of ionization is less than 1%. In spite of differences between them, both our results and those of Winter *et al.*[5] appear to be in good agreement with the experiments (though our lower values at 4 and 8 keV do seem to lie slightly closer to the data points given in Ref. 12, the error limits on the experimental data do not permit a firm conclusion as to which set of results is more accurate). More accurate measurements of this cross section, or accurate measurements of the direct excitation cross sections, would be of considerable interest for the questions discussed here.

ACKNOWLEDGMENTS

We thank the Natural Sciences and Engineering Research Council of Canada for support of this work through Operating Grant No. A-5330. Computations were performed at the University of Alberta Computing Centre using the Amdahl V/7 digital computer. We also thank Dr. T. G. Winter and Dr. G. J. Hatton for communicating some results of their work to us in advance of publication.

---

*Present address: c/o Dept. of Physics, University of Missouri, Rolla, Miss. 65401.

†Based on a doctoral thesis submitted by M. Kimura in partial fulfillment of requirements for the Ph.D. degree, University of Alberta, 1981.

[1]R. D. Piacentini and A. Salin, J. Phys. B 7, 1666 (1974); 9, 563 (1976).

[2]R. D. Piacentini and A. Salin, J. Phys. B 10, 1515 (1977).

[3]T. G. Winter and N. F. Lane, Phys. Rev. A 17, 66 (1978).

[4](a) T. G. Winter and G. J. Hatton, Phys. Rev. A 21, 793 (1978); (b) G. J. Hatton, N. F. Lane, and T. G. Winter, J. Phys. B 12, L571 (1979).

[5]T. G. Winter, G. J. Hatton, and N. F. Lane, Phys. Rev. A 22, 930 (1980).

[6]J. Vaaben and K. Taulbjerg, *Abstracts of the Eleventh International Conference on the Physics of Electronic and Atomic Collisions, Kyoto, Japan, 1979,* edited by K. Takayamagi and N. Oda (The Study for Atomic Collision Research, Kyoto, 1979), p. 566.

[7]R. E. Olson, A. Salop, R. A. Phaneuf, and F. W. Meyer, Phys. Rev. A 16, 1867 (1977).

[8]W. L. Fite, A. C. H. Smith, and R. F. Stebbings, Proc. R. Soc. London, Ser. A 268, 527 (1962).

[9]M. B. Shah and H. B. Gilbody, J. Phys. B 11, 121 (1978).

[10]W. L. Nutt, R. W. McCullough, K. Brady, M. B. Shah, and H. B. Gilbody, J. Phys. B 11, 1457 (1978).

[11]J. E. Bayfield, and G. A. Khayrallah, Phys. Rev. A 12, 869 (1975).

[12]B. Peart, R. Grey, and K. T. Dolder, J. Phys. B 10, 2675 (1977).

[13]G. C. Angel, E. C. Sewell, K. F. Dunn, and H. B. Gilbody, J. Phys. B 11, L297 (1978).

[14]J. B. A. Mitchell, K. F. Dunn, G. C. Angel, R. Browning, and H. B. Gilbody, J. Phys. B 10, 1897 (1977).

[15]D. R. Bates and R. McCarroll, Proc. R. Soc. London, Ser. A 245, 175 (1958); Adv. Phys. 11, 39 (1962).

[16]W. R. Thorson and J. B. Delos, Phys. Rev. A 18, 117 (1978); 18, 135 (1978).

[17]S. B. Schneiderman and A. Russek, Phys. Rev. 181, 311 (1969).

[18]H. Levy II and W. R. Thorson, Phys. Rev. 181, 252 (1969).
[19]C. F. Lebeda, W. R. Thorson, and H. Levy II, Phys. Rev. A 4, 900 (1971); V. SethuRaman, W. R. Thorson, and C. F. Lebeda, Phys. Rev. A 8, 1316 (1973).
[20]J. Rankin and W. R. Thorson, Phys. Rev. A 18, 1990 (1978).
[21]J. Vaaben and K. Taulbjerg (unpublished).
[22]J. B. Delos and W. R. Thorson, J. Chem. Phys. 70, 1774 (1979).
[23]W. R. Thorson, M. Kimura, J. H. Choi, and S. K. Knudson, Phys. Rev. A 24, 1768 (1981).
[24]J. B. Delos, Phys. Rev. A 23, 2301 (1981).
[25]M. Kimura and W. R. Thorson, Phys. Rev. A 24, 1780 (1981).
[26]M. Kimura, Ph.D. thesis, University of Alberta, Department of Chemistry, 1981 (unpublished).
[27]D. R. Bates and T. R. Carson, Proc. R. Soc. London, Ser. A 234, 207 (1956).
[28]R. Bulirsch and J. Stoer, Numer. Math. 8, 1 (1966).
[29]The value 0.247×10^{-16} cm^2 was obtained using straight-line trajectories, while Vaaben and Taulbjerg (Ref. 6) used the HeH^{2+} $2p\sigma$ potential curve to determine trajectories. [Dr. J. Vaaben (private communication) has confirmed that a result close to the above value is also obtained by him using straight-line trajectories.] However, the extensive studies by Winter and Lane (Ref. 3), and also some studies we have done at 1 keV, on the effects of Coulombic versus straight-line trajectories, show that these are relatively small, and we think it unlikely that the discrepancy is a trajectory effect.
[30]The resonance is exact at $R\rightarrow\infty$, but at finite distances the difference in Coulomb fields (cf. Fig. 1) makes it effectively a case of near resonance.
[31]In the course of work on H^+-H(1s) collisions (Ref. 25) we have studied effects of changes in matrix element shape and structure on (nonresonant) transition probabilities. As a rule, steeper slopes and the occurrence of sign changes in matrix elements lead to increased transition probabilties, and it is these differences in the $1s\sigma\rightarrow2p\sigma$ coupling shown in Fig. 8 which are probably responsible for the larger cross sections of Ref. 5.
[32]D. Rapp, J. Chem. Phys. 61, 3777 (1974).